

Ironmaking

The evolution of ironmaking process based on coal-containing iron ore agglomerates

W-K.LU *et al.*

Fundamentals of kinetics and mechanisms of iron oxide reduction of indurated pellets by reducing gases and of coal-containing iron ore composites, are reviewed. The gaseous products of the latter can be used to protect sponge iron from re-oxidation by a fully oxidized flame, provided the bed height of coal-containing iron ore agglomerates and the flame temperature are sufficiently high. Potential operational problems in RHF (Rotary Hearth Furnace) for tall beds and high flame temperature are discussed and a new hearth furnace, the Paired Straight Hearth (PSH) Furnace, is proposed.

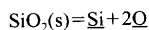
(*cf. ISIJ Int.*, 41 (2001), 807)

Fundamentals of High Temperature Processes

Deoxidation equilibrium of chromium stainless steel with Si at the temperatures from 1823 to 1923 K

K.SUZUKI *et al.*

The deoxidation equilibrium of chromium stainless steel with silicon was studied up to 25 mass% chromium at the temperatures of 1823, 1873 and 1923 K, in order to clarify the effect of chromium on silicon deoxidation of liquid iron-chromium alloys. Results obtained were summarized as follows



$$\log K_{\text{Si}} (= a_{\text{Si}} \cdot a_{\text{O}}^2 / a_{\text{SiO}_2}) = -24600/T + 8.40$$

$$\log f_{\text{Si}}^{\text{Cr}} = -0.021[\% \text{Cr}] + 4.3 \times 10^{-4}[\% \text{Cr}]^2, \\ [\text{mass}\% \text{Cr}] \leq 25, 1823 \leq T \leq 1923 \text{ K}$$

The phase stability diagrams of Si-Al complex deoxidation was estimated at [mass%Cr]=0, 13, 20 and 1823 K, by applying present results and recent data assessed by one of authors for Cr- and Al-deoxidation equilibria in liquid iron.

(*cf. ISIJ Int.*, 41 (2001), 813)

Reaction behavior of facing pair between hematite and graphite: A coupling phenomenon of reduction and gasification

Y.KASHIWAYA *et al.*

Recently, the reaction of composite pellet consisting of the iron ore and carbonaceous materials such as coal, char and coke was investigated. The fast reaction rate and relatively low starting temperature were reported by many researchers. In such a reaction condition, the mechanism of reaction will be changed during reaction from the situation that the iron ore and carbon are directly contacting and to the separate situation.

The simultaneous reaction between reduction and gasification of carbon was examined using hematite-graphite facing pair, which is to clarify the effect of reaction occurring in the separated place. From the definition of coupling phenomenon, the discussion about the 'produced energy' related to the production of entropy was carried out in view point of two aspects that were (a) the gas composi-

tion change and (b) the evolution of reaction heat.

The starting temperature of gasification decreased from 900°C to 600°C in the facing pair under CO₂ atmosphere and to 250°C under CO atmosphere. The effect of reaction heat of reduction was measured and discussed through new mechanism of reduction.

(*cf. ISIJ Int.*, 41 (2001), 818)

Steelmaking

Effect of oxide fluxes on the viscosity of molten aluminothermic ferro-chrome slags

R.C.BEHERA *et al.*

The viscous slag generated during aluminothermic reduction of metallic oxides for production of metals or alloys slows down the reduction process and obstructs clear separation of slag and metal. The fluxing constituents are added to bring down the viscosity.

Hence the effect of variation of CaO and MgO contents on the viscosity of synthetically prepared ferro-chrome slags having an approximate composition of industrial ferro-chrome slags resulting from aluminothermic reduction of chromium oxide has been studied at various temperatures. Increase of CaO and MgO contents is found to decrease the viscosity of the slags. The relative decrease in viscosity becomes very less beyond 40 mol% of CaO. It is further observed that both CaO and MgO additions do not decrease the viscosity appreciably at higher temperatures as they do at lower temperatures.

The activation energy of viscous flow calculated from the viscosity data, is seen to obey the Arrhenius equation ($\mu = A_0 \exp(E_\mu/RT)$). The activation energy, E_μ decreases with increased flux addition. It is also observed that the activation energy of viscous flow is independent of temperature but is a function of the composition of the slag. Within the range of compositions studied, the net-work breaking ability of Mg²⁺ ion is not as high as that of Ca²⁺ ion. The possible ionic structure of the liquid slags and ionic interactions have been discussed in light of the calculated values of activation energy of viscous flow. Al₂O₃ does not behave as an amphoteric oxide as it does in silicate melts.

(*cf. ISIJ Int.*, 41 (2001), 827)

Viscosity of molten Al₂O₃-Cr₂O₃-CaO-CaF₂ slags at various Al₂O₃/CaO ratios

R.C.BEHERA *et al.*

Calcium fluoride, known as fluor spar is a very good flux in steel making and also has been reported to increase the alloy yield and metal recovery in aluminothermic melts for production of ferrochrome. The present investigation is therefore carried out to study the effect of CaF₂ additions on the viscosity of synthetically prepared aluminothermic slags pertaining to the production of ferrochrome, with the composition approximating that of ferrochrome slag generated in the industry. The viscosities of these slags have been measured at four different Al₂O₃/CaO ratios with the broad composition of the slags varying between 50–62 mass% Al₂O₃, at various temperatures.

Calcium fluoride additions decreased the viscosity of aluminothermic ferrochrome slags at all temperatures. It is observed that the decrease in viscosity is different at different Al₂O₃/CaO ratios and that at all temperatures there is fast decrease in viscosity initially at lower CaF₂ contents, the rate of decrease diminishing at higher mole percent of CaF₂. The viscosity is found to obey the Arrhenius equation of viscous flow at two different temperature ranges and not throughout the temperature range above liquidus.

The activation energy at the two temperature ranges have been estimated and it is found to be strongly dependent not only on the CaF₂ content but also on the Al₂O₃/CaO ratio.

From the analysis of results it is suggested that the decrease of viscosity with increasing additions of CaF₂ content may be due to both depolymerisation and decreasing intensity of interactions among various anions and cations in the melt.

(*cf. ISIJ Int.*, 41 (2001), 834)

Casting and Solidification

Effect of static magnetic field application on the mass transfer in sequence slab continuous casting process

B.LI *et al.*

A mathematical model has been developed to analyze the mass transfer in the sequence continuous casting process with the static magnetic field. The induced electromagnetic force is obtained by solving simultaneous equations for the momentum and the electromagnetic field. The application of static magnetic field affects the mass transfer by changing the flow field in the strand. The results of numerical calculation show a reasonable agreement of the calculated relative concentration of mixed steel with the measured one. The mixing of molten steel in the low part of the mold is significantly suppressed by the static magnetic field, and composition of new grade steel along the slab length in the transition zone increases significantly. The distribution of relative concentration averaged at cross section changes from parabolic to integral symbolic-like along the slab length, and the transition length is reduced about 50% by applying the magnetic field of 0.5 T.

(*cf. ISIJ Int.*, 41 (2001), 844)

Fluid flow in a continuous casting mold driven by linear induction motors

K.OKAZAWA *et al.*

Numerical flow analyses are performed to clarify the characteristics of a molten steel flow in the continuous casting mold using the electromagnetic stirring. The usage and variables of the linear induction motor in electromagnetic stirring are noted in the analysis. Uniformity of the circulating flow velocity is examined quantitatively. Especially, influences of the installed level of the linear induction motor which is one of the most important usage of the linear induction motor, and the pole number, which is one of the most important linear induction motor variables, on the molten steel flow are intruded.

(*cf. ISIJ Int.*, 41 (2001), 851)

Forming Processing and Thermomechanical Treatment

Effects of tempering temperature on wear resistance and surface roughness of a high speed steel roll

J.H. LEE *et al.*

The effects of tempering temperature on wear resistance and surface roughness of a high speed steel (HSS) roll manufactured by centrifugal casting method were investigated in this study. Hot-rolling simulation test was carried out using a high-temperature wear tester capable of controlling speed, load, and temperature. The test results revealed that the peak-tempered roll specimen showed the best wear resistance because of its hard matrix. However, its surface roughness deteriorated as the scratching wear proceeded, thereby leading to increase in friction coefficient. In the over-tempered specimens containing numerous fine spherical carbides in the matrix, the abrasive wear occurred predominantly as fine carbides were fallen off from the matrix, and thus the surface roughness was enhanced by the homogeneous wear of both matrix and carbides. These findings suggested that the tempering treatment at temperatures slightly past the peak hardness point would be more desirable in order to improve the wear resistance with consideration of the surface roughness of the HSS roll.

(*cf. ISIJ Int.*, **41** (2001), 859)

Transformations and Microstructures

A kinetic and electronmicroscopic study of transformations in continuously cooled Fe-15%Ni alloys

E.A. WILSON *et al.*

Koistinen and Marburger's equation relating volume fraction of athermal martensite to temperature has been applied to diffusional transformation dilatometry data obtained on continuous cooling Fe-15%Ni alloys. After austenitising for 1 h at 1000°C and cooling at 50 K/min (0.83 K/s), grain boundary nucleated massive ferrite was observed which developed into Widmanstätten ferrite with a ferrite habit plane of $\{110\}_b$ for temperatures between 372°C and 352°C. On cooling at 44 K/s from 1000°C bainitic ferrite was observed for temperatures below 360°C. There was some retained austenite in this bainitic structure giving a ferrite habit plane of $\{110\}_b$ parallel to the austenite plane $\{111\}_r$. Cooling at the same rate, 44 K/s from 1200°C gave lath martensite below the M_s of 261°C with a ferrite habit plane of $\{112\}_b$. Superlattice spots corresponding to the DO₃ or B2 structure were observed in electron diffraction patterns on cooling at 50 K/min (0.83 K/s) and 44 K/s from 1000°C.

(*cf. ISIJ Int.*, **41** (2001), 866)

Influence of hot deformation conditions on the annealing behaviour of cold rolled ultra low carbon steel

M. FERRY *et al.*

An ultra low carbon (ULC) steel has been de-

formed in plane strain compression (PSC) using a Gleeble 3500 thermal and mechanical simulator followed by cold rolling and annealing (CRA). Multiple-pass deformation was used to simulate conditions encountered during hot rolling and to study the effect of finish deformation temperature (FDT) on microstructural development during CRA. It was found that a range of ferrite microstructures were produced when FDT decreased from 920 to 600°C, a temperature range which encompasses both austenite (γ) and ferrite (α) deformation. For FDT > 870°C, fine equiaxed ferrite was produced, whereas FDT ~ 850°C produced a coarse-grained microstructure. As FDT was decreased below 850°C, as-deformed ferrite remained with a decreasing propensity for the formation of statically recrystallized grains. At higher FDT, the γ -to- α transformation produced a hot-band texture consisting mainly of $\{001\}\langle 110 \rangle$, and at FDT below the critical transformation temperature the typical body centred cubic rolling texture also developed. Sections of the as-hot-deformed samples were cold rolled to 80% reduction and annealed at 650°C. It was found that the hot deformation microstructure has a strong influence both on the kinetics of recrystallization and texture development during CRA. In particular, a warm-deformed ferrite microstructure (lower FDT) recrystallized most rapidly to produce a strong $\langle 111 \rangle // ND$ recrystallization texture (γ -fibre), whereas an initial coarse-grained ferrite microstructure recrystallized most sluggishly to produce a strong $\{001\}\langle 110 \rangle$ texture. The implications of these results in the production of formable sheet steels is outlined.

(*cf. ISIJ Int.*, **41** (2001), 876)

Recrystallization of a cold rolled trip-assisted steel during reheating for intercritical annealing

R. PETROV *et al.*

A TRIP-assisted steel, with a conventional composition containing 0.11% C, 1.53% Mn and 1.26% Si, and a hot band microstructure composed of ferrite, martensite and carbide particles, was cold rolled with a reduction of 70%. Partially recrystallized samples were obtained by water quenching the cold rolled sheets which were reheated at a constant rate of 10°C/s to temperatures in the range between 525°C (<A_{c1}) and 800°C (>A_{c3}). It was demonstrated that the recovery and recrystallization behaviour was critically controlled by the carbide formation and growth during the initial stages of the annealing treatment. No interaction was observed between recrystallization and transformation phenomena as the static recrystallization was already completely finished before the start of the $\alpha \rightarrow \gamma$ phase transformation. The microtexture observations obtained by orientation imaging microscopy have revealed that the $\langle 111 \rangle // ND$ fibre which dominates the annealing texture at the end of the static recrystallization already starts to develop at the initial nucleation stage. The $\{111\}\langle 110 \rangle$ fibre component which is slightly favoured in the recrystallization texture together with other less common BCC annealing components quickly disappear from the ferrite texture after the start of the phase transformation, which could be related to the preferential presence of redis-

solving carbide particles in these components.

(*cf. ISIJ Int.*, **41** (2001), 883)

Simulation of hot-band microstructure of C-Mn steels during high speed cooling

M. THOMPSON *et al.*

The evolution of microstructure in a range of C-Mn steels during hot strip rolling and subsequent high speed cooling was simulated by quench dilatometry using cooling rates up to 600°C/s. The influence of coiling temperature on the microstructure and mechanical properties of the hot band was also investigated by interrupted cooling experiments. Continuous cooling transformation (CCT) diagrams for a range of cooling schedules were constructed for each steel where it was found that rapid cooling lowers significantly the Ar₃ temperature, refines the ferrite to grain sizes in the range 3–6 μ m and increases the hardness. An increase in Mn content (mass %) from 0.45 to 1.0% lowers the Ar₃ temperature, retards the rate of $\gamma \rightarrow \alpha$ transformation and promotes the formation of non-equilibrium phases. The role of alloying additions, in combination with cooling rate and coiling temperature is discussed in the context of microstructural development and strengthening of as-hot-rolled C-Mn strip.

(*cf. ISIJ Int.*, **41** (2001), 891)

Mechanical Properties

Effect of morphological change of carbide on elongation of boron-bearing Al-killed steel sheets

Y. FUNAKAWA *et al.*

It has been reported that boron has a beneficial effect on the mechanical properties of continuously annealed Al-killed steel sheets. However, the effect of boron on elongation of boron-bearing steels had not been fully investigated. In this study, the effect of boron on elongation was investigated for boron-bearing Al-killed steel sheet by analyzing the substantial effects of fine carbides precipitating in matrix and at the grain boundaries.

Using scanning electron microscope and image analyzer, an investigation was made for the precipitation site and the size distribution of fine carbides caused by the variation of excess boron and overaging temperature. The effects of fine carbides on the tensile elongation of the steels were examined. The carbide morphology and the precipitation site changed with excess boron since the excess boron accelerated carbide precipitation in matrix by segregating at the grain boundaries. In the case where uniform elongation and post-uniform elongation were evaluated by n -value and m -value respectively, n -value decreased with increasing amount of fine carbides in matrix. Furthermore, excess boron deteriorated n -value irrespective of carbide morphology. On contrast, m -value rose with a decrease in the diameter of carbide at the grain boundary irrespective of small amount of excess boron. It was indicated that the deterioration of elongation by the small amount of excess boron was caused by a decrease in uniform elongation, which might be attributed to fine carbides in matrix and boron in solution.

(*cf. ISIJ Int.*, **41** (2001), 900)

Precipitation behavior of NbC in 9%Cr1%Mo0.2%VNb steel

M. TAMURA *et al.*

Dissolved Nb in both austenitic and ferritic phases of 9%Cr1%Mo0.2%VNb steel was measured using an inductively coupled plasma atomic emission spectroscope (ICP), and the microstructure has been characterized using a field emission scanning electron microscope of a ultra high resolution type and an analytical electron microscope. The dissolved Nb in austenitic phase measured by ICP is in agreement with that predicted by a phase equilibrium calculation system. However, the measured values of dissolved Nb in the specimens which are heat-treated for 2 h just below A_{C1} are much higher than the calculated values. It is newly confirmed by both chemical and physical analyses that the fine NbC particles which are preformed at 950°C and stable at this temperature are on one occasion re-dissolved into the matrix by the subsequent heat treatment at 800°C for 2 h. This fact suggests that high temperature tempering is recommended in order to improve creep resistance of high Cr heat resisting steels which contain strong carbo-nitride formers.

(*cf. ISIJ Int.*, **41** (2001), 908)

Modelling of interaction between creep and oxidation behaviour for engineering materials

N. ROY *et al.*

Mechanical test data for design of high temperature components are mainly collected from tests conducted in air even though these are used in different environment. Therefore, in order to predict accurately the performance of a component in actual service it is necessary to develop appropriate constitutive equations taking into consideration the environmental effect. The paper briefly describes how our current knowledge on Continuum Damage Mechanics (CDM) can be utilized to formulate the same. In absence of sufficient experimental data, most of the existing approaches provide only qualitative support for their models. Creep test on specimens having different section sizes, under identical conditions, can provide valuable information on creep/environment interaction. A simple analytical method has been developed to extract the material parameters determining the kinetics of environmental attack from a creep strain-time plot. It has been shown that the material constants thus obtained provide good explanation of the observed section size and geometry effects in steels and nickel base superalloys.

(*cf. ISIJ Int.*, **41** (2001), 915)

Microstructural evolution during creep test in 9Cr-2W-V-Ta steels and 9Cr-1Mo-V-Nb steels

T. HASEGAWA *et al.*

In order to clarify the mechanism of remarkable creep strength of the 9Cr-2W-0.2V-Ta steels, high-Cr heat-resistant steels with Mo replaced by W and Nb by Ta for reducing induced radioactivity, the microstructural evolution during creep tests has been studied and compared with that in conventional 9Cr-1Mo-0.2V-Nb steels. Particular attention was called to quantitative analysis of solute W and Mo contents evaluated with the EDX spectra measured with the thin foil in the FE-TEM analysis.

It has been supposed that the martensitic microstructure and fine MX-type precipitates have no significant effect on the difference in creep properties between the W-containing steel and the Mo-containing steel.

Moreover the creep strength of the W-containing steel can not be attributed to the larger solid solution hardening by W. Mo distribution may encourage creep strain localization in solid solution, which results in the deterioration of creep strength of Mo-containing steels. Comparing $M_{23}C_6$ and Laves phase, the latter is assumed to be the main governing factor.

(*cf. ISIJ Int.*, **41** (2001), 922)